Journal Name

ARTICLE

Association and Relaxation of Supra-Macromolecular Polymers.

Stephen C. Boothroyd,[a] David M. Hoyle,[a] Thomas C.B. McLeish,[b] Etienne Munch,[c] Regis Schach,[c] Andrew J. Smith,[d] and Richard L. Thompson[a]

Received 00th January 20xx,
Accepted 00th January 20xx

DOI: 10.1039/x0xx00000x

www.rsc.org/

This paper describes the structures created by assembling functionalised entangled polymers and the effect these have on the rheology of the material. A polybutadiene (PBd) linear polymer precursor of sufficient molecular weight to be entangled is used. This is end functionalised with the self-associating group 2-ureido-4pyrimidinone (UPy). Interestingly, despite the relatively high molecular weight of the precursor diluting the UPy concentration, the effect on the material's properties is significant. To characterise the assembled microstructure we present linear rheology, extensional non-linear rheology and small angle X-ray scattering (SAXS). The linear rheology shows that the functionalised PBd assembles into large macro-structures where the terminal relaxation time is up to seven orders of magnitude larger than the precursor. The non-linear rheology shows strain-hardening over a broad range of strain-rates. We then show by both SAXS and modelling of the extensional data that there must exist clusters of UPy associations and hence assembled polymers with branched architecture. By modelling the supra-molecular structure as an effective linear polymer, we show that this would be insufficient in predicting the strain-hardening behaviour at lower extension-rates. Therefore, in this flow regime the strain-hardening is likely to be caused by branching. This is backed up by SAXS measurements which show that UPy clusters larger than pair-pair groups exist.

1 Introduction

Polymers functionalised with reversibly associative substituents, driven by non-covalent interactions, have gained much interest in recent years[1–15] in a variety of materials science applications. These include reversible blending of immiscible polymers,[16] self-healing,[17–19] improved processability[4,20,21] and smart adhesive surfaces.[22–24] This is driven by the ability of such polymers to assemble into a number of well-defined morphologies with enhanced properties.

The structure of the functional groups is key to the assembly of the polymers. Ionomers are polymers with ionic groups capable of forming physical networks through hydrogen bonding or ionic interactions when neutralized with counter ions, and have gained much interest in this area.[25] Stadler and co-workers[6,26] have investigated the rheological properties of such materials, polybutadienes (PBds) telechelically functionalised with carboxylic acid groups, which form a network structure when neutralised with metal cations. They found a number of interesting effects important to the processing and properties of the materials, including an extension of the terminal relaxation time by seven decades, and strain hardening under extension. The behaviour of these systems is however highly dependent on the nature of the counterion clusters dispersed within the polymer.

Hydrogen bonding groups have been particularly well studied, with different functionalities such as nucleo bases and their analogues,[15,23,24,27–29] diaminotriazine,[27,28] acrylamidopyridine,[30] acrylic acid[30] and carboxyethylacrylate[30] amongst others. Various studies have also looked at systems with two hydrogen bonding groups, where complementary interactions may be more favourable than self-complementary interactions.[15,27,29] One functional group that has gained particular attention is 2-ureido-4-pyrimidinone (UPy) (Fig. 1). First used to functionalise polymers by Sijbesma and Meijer,[31] this motif is capable of forming four hydrogen bonds, and as such has a high dimerization constant (> 10^7 M^{-1} in chloroform[32]). While the association of multiple hydrogen bonding moieties has been shown to be sensitive to environmental conditions and decreases with increasing humidity[33], it is accepted that these groups are strongly associating unless there are competing hydrogen bonding species present. The strength of hydrogen bonding has been shown to be hugely important to the rheological properties of the functionalised polymer,[11,30,34] as well as the temperature for dissociation of the H-bonding group and therefore material processing.[34] Well defined fibre morphologies driven by stacking of UPy dimers have been seen for polymers with additional urea or urethane linkers built into the telechelic

[a]*Department of Chemistry, Durham University, Lower Mountjoy, South Road, Durham DH1 3LE, U.K.*

[b]*Department of Physics, University of York, Heslington, York YO10 5DD, U.K.*

[c]*Manufacture Française des Pneumatiques Michelin, Centre de Technologies, 63040 Clermont Ferrand cedex 9, France*

[d]*Diamond Light Source Ltd., Diamond House, Harwell Science and Innovation Campus, Didcot, U.K.*

† Footnotes relating to the title and/or authors should appear here.
Electronic Supplementary Information (ESI) available: [details of any supplementary information available should be included here]. See DOI: 10.1039/x0xx00000x

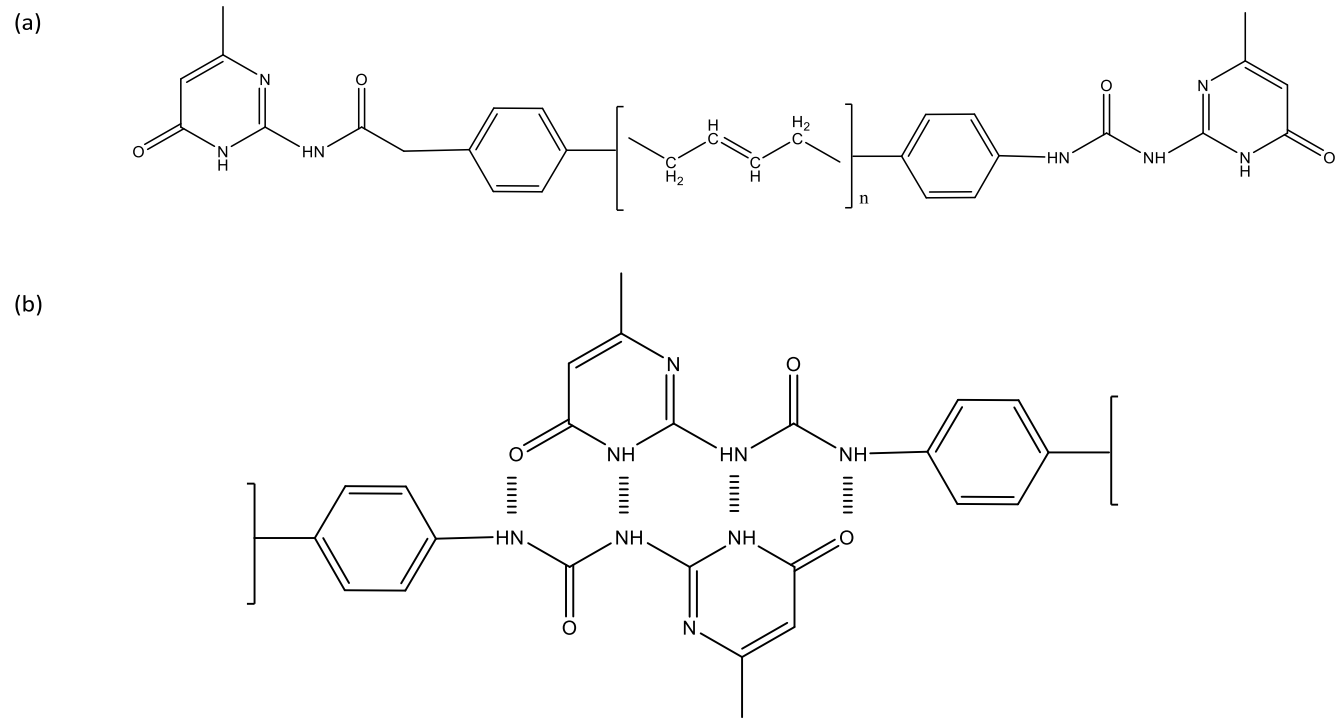

Fig. 1 (a) Sketch of UPy functionalised telechelic PBd, (b) Assembly into dimer via four hydrogen bonds.

functionality.[2,3] Botterhuis et al., have shown that such phase separation can also be driven by UPy groups without such additional functionalities if the incompatibility of the UPy group with the polymer is high enough.[14] It was also shown that the length of the polymer chain is important in determining the morphology of the phase separated structure, while Appel et al. have used different substituents on the UPy group to control nanofibre formation and crystallisation rates.[2]

Here we study the effect of UPy groups on the rheological behaviour of telechelically functionalised, entangled PBds (Fig. 1). While much work has been done studying the self-assembly of these materials in polymers below their entanglement molecular weight, M_e, less has been done on systems above M_e. The significance of entanglement on rheology is not trivial to predict. Jangizehi et al. have very recently reported that the presence of UPy groups on functionalised polymers has significantly less impact on diffusion than molecular weight.[10] On this basis, it might be expected that the impact on rheology is quite small. However, Ishiwari et al. have shown that some functional groups can cause significant structural organisation, even in relatively large polymers.[9] Our UPy end-functionalised polymers are expected to assemble end to end via hydrogen bonding of the UPy groups. The prospect of assembling polymer chains with a much higher effective M_w is desirable for multiple applications. Polymers with extremely high molecular weights are problematic to process because of their long relaxation times, often of order 10^3 s. To avoid this problem it would be desirable to synthesise a polymer which can assemble into a chain with the enhanced properties of a relatively high molecular weight at ambient temperatures, but which falls apart at processing temperatures. We characterise the effect of the UPy groups on the rheological properties of the polymers. This includes linear oscillatory rheology, and non-linear extensional rheology. We find that the UPy groups have a remarkable effect on both the linear relaxation of the PBds, and on their non-linear extensional properties. Supported by small-angle X-ray scattering results, we are able to develop a constitutive model to characterise the architecture of the self-assembled structure formed by these polymers from the rheological behaviour. In addition, we investigate the importance of chain microstructure and molecular weight to the assembly and properties of the PBds.

2 Materials and Methods

2.1 Synthesis of telechelic amine functionalized PBd

5 L of methylcyclohexane was introduced into a reactor (10 L) and mixed with 335 g of butadiene. The mixture was warmed to 50 °C and then 20 mmol of 4-lithium-N,N-bis(trimethylsilyl)aniline in solution in methylcyclohexane (200 mL) was added in order to initiate the polymerization of butadiene. When monomer conversion reached 100%, the living polybutadienyl chains were coupled with dimethyldichlorosilane (0.45 equivalents per Li) at 50 °C for 15 min. An antioxidant was added to the polymer solution and then the polymer treated with hydrochloric acid at 37 wt. % (2 equivalents per Li) in 5 L of water for 96 h at 90 °C to generate the primary amine. The polymer solution was then washed with demineralized water until the pH was equal to 7. The solvent was then removed under reduced pressure in an oven at 60 °C.

2.2 Synthesis of telechelic UPy functionalized PBd

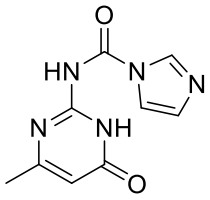

Fig. 2 UPy (1H-Imidazole-1-carboxamide, N-(1,6-dihydro-4-methyl-6-oxo-2-pyrimidinyl)-).

11.2 g of telechelic amine functionalized PBd was solubilized in 150 mL of dichloromethane and mixed with 552 mg of UPy (Fig. 2, 56 mmol, 205 g mol^{-1}). After 48 h at 40 °C, 97% molar of primary amine had reacted with UPy. The solvent was then removed under reduced pressure in an oven at 60 °C. The reaction between the telechelic amine functionalized PBd and UPy was followed by NMR ^{1}H. Table 1 summarises the molecular weight and microstructural data of the six polymers used in this study. Polymer M_w was determined by size exclusion chromatography (SEC), using a Viscotek TDA 302 instrument. Tetrahydrofuran was used as the eluent at a flow rate of 1 mL min^{-1}, and the M_w calibrated with PBd standards (see supporting information Fig. S1).

The glass transition temperature (T_g) of the polymers was determined by differential scanning calorimetry (DSC), using a TA instruments Q1000. Samples were subjected to a heating and cooling cycle at a rate of 10 °C min^{-1} from -90 – 180 °C. The T_g was taken as the inflection point of the heat flow curve, analysed using the TA Universal Analysis software (see supporting information Fig. S2).

2.3 Sample pressing

Samples were pressed for rheometry or small angle X-ray scattering at a temperature of 25 °C for 30 mins and a force of 6 tons. This pressing time exceeds the terminal relaxation time of 1450 s for UPy1 at 25 °C.

2.4 Rheometry

Linear torsional rheometry was conducted on a TA instruments AR 2000 rheometer equipped with either a Peltier plate or environmental testing chamber with nitrogen gas inlet. Parallel plate geometries were used with either 25 mm or 8 mm diameter dependent on the polymer sample being studied. Strain sweeps were conducted prior to frequency measurements to ensure tests were conducted within the linear viscoelastic region. Frequency measurements were then conducted at a strain of 1% between 0.1-100 Hz. Extensional rheology was conducted using the Sentmanat Extensional Rheometer 2 add-on. Samples of width 10 mm and thickness 0.5 mm were pressed and tested at a variety of extension rates, at 25 °C.

Table 1 Summary of molecular weight and microstructural data for functional polymers and their counterparts.

Polymer	M_w / Da	M_n / Da	Telechelic group	T_g / °C	1,4 %
UPy1	27,800	21,000	UPy	-39.6	35
Am1	27,200	20,300	NH_2	-40.2	35
UPy2	32,900	27,800	UPy	-79.9	76
Am2	28,200	25,300	NH_2	-81.9	76
UPy3	193,200	132,600	UPy	-76.1	79
Am3	84,600	70,300	NH_2	-76.3	78

2.5 Small angle X-ray Scattering (SAXS)

SAXS experiments were conducted on beamline I22 at Diamond Light Source. Samples of UPy1, 2 and 3, and Am1 and 3 were mounted in a Linkam DSC hot stage, in pans with mica windows. Measurements were conducted in the q range 0.0074-0.4894 Å^{-1} using a beam energy of 12.4 keV and a sample detector distance of 3.2619 m. Each dataset was corrected for transmission, the empty beam and background scattering, and placed on an absolute scale using the scattering from a glassy carbon standard. The data were fitted as described in the results and discussion using SasView.[35] Complementary SAXS measurements were carried out on Am2 in-house at Michelin, Clermont Ferrand, and corrected for transmission, the empty beam and background scattering, and placed on an absolute scale using a glassy carbon standard.

3 Results and Discussion

Rheological master curves of the polymers were produced by measuring the frequency dependent behaviour at a range of temperatures. In the first instance, data were then shifted using Reptate[36] according to the time temperature superposition (TTS) theory of Williams-Landel-Ferry[37] (WLF). Initially Reptate reference values for PBd were used, before fitting these values to the functionalised polymer rheology. Several key differences can be seen when comparing the rheological properties of UPy1 and Am1 (Fig. 3a), which differ only in their end-functional groups. UPy1 displays a huge extension of the terminal relaxation crossover time compared to that of Am1. For Am1 this corresponds to a frequency of ~8560 rad s^{-1} and hence a time of ~1.2×10^{-4} s with the reference temperature fixed as 25 °C. For UPy1 the terminal relaxation time is ~1450 s extending the crossover time by seven orders of magnitude compared to that of Am1. This is similar to that observed for carboxylated PBds neutralised with cations.[38] In addition to this huge increase in the terminal relaxation time of the polymer, it is also apparent from Fig. 3(a) that there is also an increase in the plateau modulus, G_N^0, of UPy1 compared to Am1. The plateau modulus is a function of the polymer entanglement density[39] and such an increase shows an increase in the number of cross-links within the system – perhaps through clustering of the telechelic groups, as shown for other rubbery telechelic polymers,[6,40] or an increase in the entanglement density of the polymer. Given the increase in the plateau modulus, this shows that on the measured time scale the association of the UPy

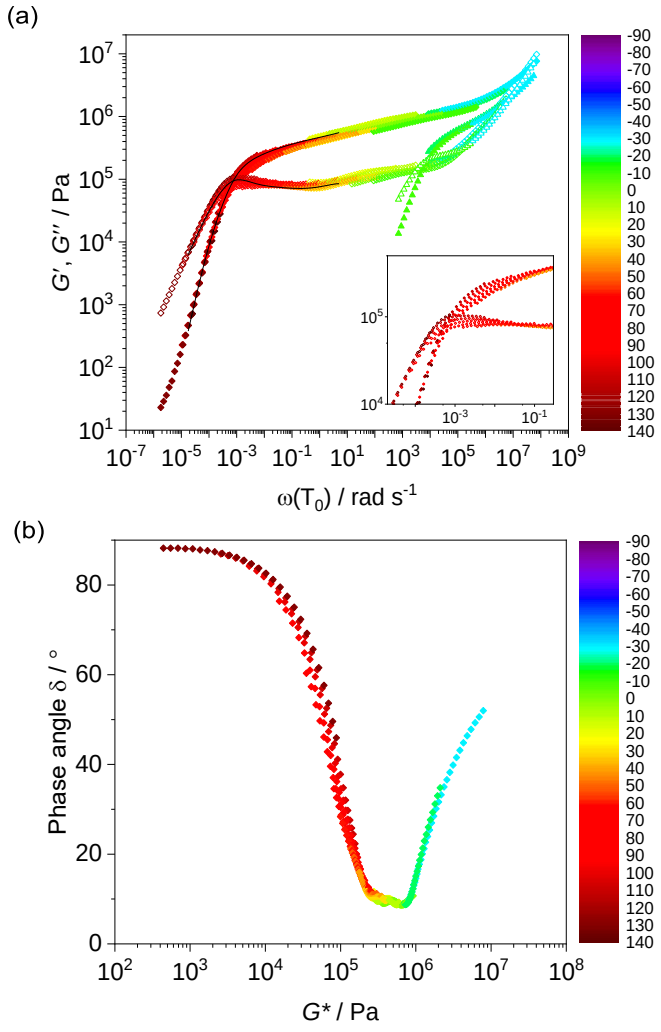

Fig. 3 (a) Rheology master curves for UPy1 (◆) and Am1 (▲) shifted using WLF theory. *G′* solid symbols, *G″* open symbols. Colour scale corresponds to the temperature of measurement, in degrees celcius. Maxwell mode fit shown with black lines. Inset highlights fanning of the TTS of UPy1 at the terminal region. T_0=25 °C. (b) van Gurp-Palmen plot of UPy1.

groups behave like permanent bonds, increasing the plateau modulus, as discussed in the work of Gold et al.[41]

As well as an increase in G_N^0, a shoulder in *G″* within the rubbery plateau of UPy1 is also apparent, at a frequency of ~100 s^{-1}, corresponding to a time scale of ~0.01 s. This is absent from the rheological data of Am1, and indeed that for standard linear PBds. Such a shoulder has also been observed in other telechelic systems,[6,8] and is indicative of the association lifetime of the interactions of the UPy group, and the time required to find a new binding partner.[41] This relaxation can also be observed in the van Gurp-Palmen plot (Fig. 3a) as a small peak as the phase angle approaches its minimum. A breakdown in the TTS shift of UPy1 can be seen at the terminal relaxation time of the network, indicated by a distinct 'fanning' of this network relaxation (Fig. 3a, inset). This shows a thermorheological complexity caused by dissociation of the UPy groups. Fanning is also observed within the rubbery plateau, towards the minimum in *G″*, and is consistent with other self-associating systems.[6,40] This fanning is also apparent in the van Gurp-Palmen plot (Fig. 3b), both in the terminal region (low moduli, high phase angle), and plateau region (towards the minimum in the phase angle). Note that the peak in *G″* at the terminal cross-over, which appears at higher temperatures (Fig. 3a, inset), has a different characteristic shape to the corresponding lower temperature data. This implies the source of fanning in the TTS could not be accounted for by any temperature or frequency shift, this includes modified TTS models such as by Zhang et al.[42] Despite this the shift gives a good representation of the rheological behaviour of UPy1, which is of the same order as the terminal relaxation time inferred from a single temperature creep recovery experiment (see supporting information Fig. S3).

Table 2 Material Parameters for Am1 calculated using the polydisperse double reptation theory in RepTate, at T_g

τ_e	1.83 s
G_N^0	1.15 MPa
M_e	1990 Da

The terminal behaviour of UPy1 shows a power law scaling of 1.5 and 0.9 for *G′* and *G″* respectively, rather than the expected exponents of 2 and 1. This shallowing in gradient would normally be associated with polydispersity in unfunctionalised polymers, but here it is possible that a range in effective molecular weight distribution arising from association is responsible.[43] For poly(*N*-isopropy- lacrylamide) gels, functionalized along the polymer chain to form cross-links, Seiffert[44] showed that the presence of sticky groups can decrease the gradient of *G′* and *G″* in the terminal region even more in polydisperse polymers. However, in our case we also see that Am1 has power law scaling of 1.4 and 0.9, so this shallowing appears to be an effect of the polydispersity in the polymers, rather than a consequence of the presence of the UPy groups.

At the crossover, the system changes from an entangled rubber, to a liquid, and for a conventional polymer the time scale at which this occurs is determined by the number of physical cross-links in the system, i.e. entanglement density. This in turn is related to the aggregation of the UPy groups on the polymer.

To understand further how the addition of the UPy group has changed the rheology of the polymer we can make a simple comparison by asking what M_w of PBd would be expected to result in a reptation time, τ_D, that corresponds to that of the cross-over time observed for UPy1? We can do this using linear theory, where τ_D can be related to the Rouse time of one entanglement segment, τ_e, by the relation: [39]

$$\tau_D = 3\tau_e Z^3 \left(1 - \frac{2C_1}{\sqrt{Z}} + \frac{C_2}{Z} + \frac{C_3}{Z^{3/2}}\right) \quad (1)$$

where:

$$Z = \frac{M_w}{M_e} \quad (2)$$

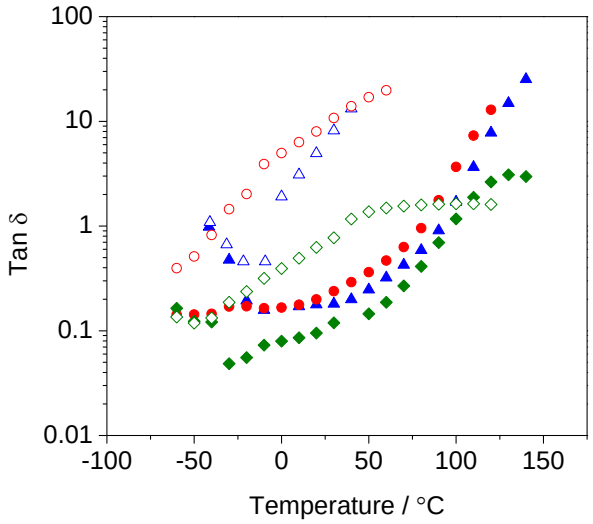

Fig. 4 Evolution of tan δ as a function of temperature for UPy1 (▲), 2 (●) and 3 (◆), and Am1 (△), 2 (○) and 3 (◇), at a frequency of 1 Hz. The low temperature rise in tan delta, particularly for UPy1 and Am1 is a consequence of the T_g of the polymer.

and C_1, C_2 and C_3 are constants with values 1.69, 4.17 and -1.55 respectively. [39] The Rouse time, τ_R, of a linear polymer is related to the number of entanglements (Z) by: [39]

$$\tau_R = \tau_e Z^2 \quad (3)$$

Hence an increase in the molecular weight of the polymer chain results in an increase in the number of entanglements in the system, and the reptation time. Such an increase, as observed here for UPy1 when compared to that of Am1, shows that UPy1 behaves as a polymer with a much higher M_w.

To estimate the effective M_w of a PBd which has a reptation time that can be compared with the terminal relxation of UPy1 it is necessary to determine τ_e. As UPy1 and Am1 share the same polymer chain and only differ in the end groups, τ_e should be the same for both polymers. τ_e can be determined for Am1 using the theory of polydisperse double reptation[39,45–48] in the RepTate program.[36] The theory accounts for polydispersity effects on the viscoelastic behaviour of the polymer, as determined from the molecular weight distribution found by SEC. From this the material parameters τ_e, M_e and G_N^0 can be determined and are shown in Table 2. The calculated values for M_e and G_N^0 are within the reported range of values for polybutadienes in the literature.[49] Taking the value of τ_e to be 2.9×10^{-7} s, the M_w can be estimated using equations 4 and 5 to be of the order ~2,400,000. This is 86 times the M_w of UPy1. If UPy1 were to assemble linearly end to end to this extent, that would suggest ~99% of UPy groups have associated.

The evolution in behaviour of all six polymers can be seen in Fig. 4, which shows the change in the tangent of the phase angle, δ, as a function of temperature at a frequency of 1 Hz. When tan δ increases above one, $G'' > G'$ and the material crosses into the terminal regime. This occurs at the lowest temperature for Am2, at ~-37 °C. Although Am1 has a slightly lower molecular weight than that of Am2, it has higher vinyl content, and therefore a raised T_g. For this reason the crossover temperature is raised to ~-5 °C. For Am3, this transition rises to ~35 °C, a consequence of the increased M_w of the polymer and an increased number of entanglements in the system. For UPy1, 2 and 3 the cross-over occurs at temperatures of ~91, 80 and 96 °C respectively. In each case the cross-over temperature is raised beyond that of its NH2 functionalised counterpart, with the biggest difference observed between that of UPy2 and Am2. The increase in crossover temperature cannot be explained by an increase in the T_g of the UPy functionalised polymers compared to their NH2 functionalised counterparts, as no significant change is detected by DSC (Table 1). It should be noted that the M_w of UPy3 measured by SEC is much greater than that of Am3 (Table 1), but this suggests that the highest M_w UPy polymer has dimerized in the SEC solvent. The UPy polymer is synthesized from the amine functionalised pre-cursor polymer, and the M_w is approximately double that of Am3. The similarities in temperature for the flow point between UPy1, UPy2 and UPy3, despite the large changes in vinyl content and M_w between the three polymers, indicate that this temperature is linked to the association of the UPy groups on the polymer. Yamauchi et al. have previously shown using rheometry that for short chain, telechelic polyisoprene functionalised with UPy that dissociation occurs at 80 °C in the polymer melt.[4]

The rheological behaviour of polymers under extension can also be highly instructive about the structure of a sample. Under extension strain hardening describes the situation when the extensional viscosity rises above that of the linear slow-flow prediction. Typically this occurs for branched and not linear or star polymers. The extensional viscosity of UPy1 was measured across a range of extension rates. It was not possible to measure the extensional properties of UPy2 and UPy3 due to break up of the sample on the extensional rheometer attachment. As this was not a problem with UPy1 it is probable that this was a consequence of the difference in chain microstructure between UPy1 and UPy2 and 3, rather than because of the presence of the UPy groups. To determine the predicted linear extensional viscosity of UPy1, TTS data were fitted at a temperature of 25 °C in RepTate[36] using twelve Maxwell modes, equally spaced on a logarithmic axis, to model the linear viscoelastic spectrum. This was then used to model the envelope for the linear extensional viscosity of the polymer as a function of time, at a temperature of 25 °C, where this is given by the Trouton relation in the limit of slow extension and shear rates:[50]

$$\eta_E(\dot{\varepsilon}) = 3\eta(\dot{\gamma}) \quad (4)$$

where η_E is the extensional viscosity, η is the shear viscosity, and $\dot{\varepsilon}$ and $\dot{\gamma}$ are the extensional and shear strain rates respectively. This prediction is shown in Fig. 5(a) as the grey symbols. Strain hardening is measured as a deviation from this behaviour and is only possible in linear polymers if the extension rate $\dot{\varepsilon} > \tau_R^{-1}$ which is the requirement for chain stretching. This can be determined by use of the Weissenberg number, W_i:

$$W_i = \dot{\varepsilon}\tau_R \quad (5)$$

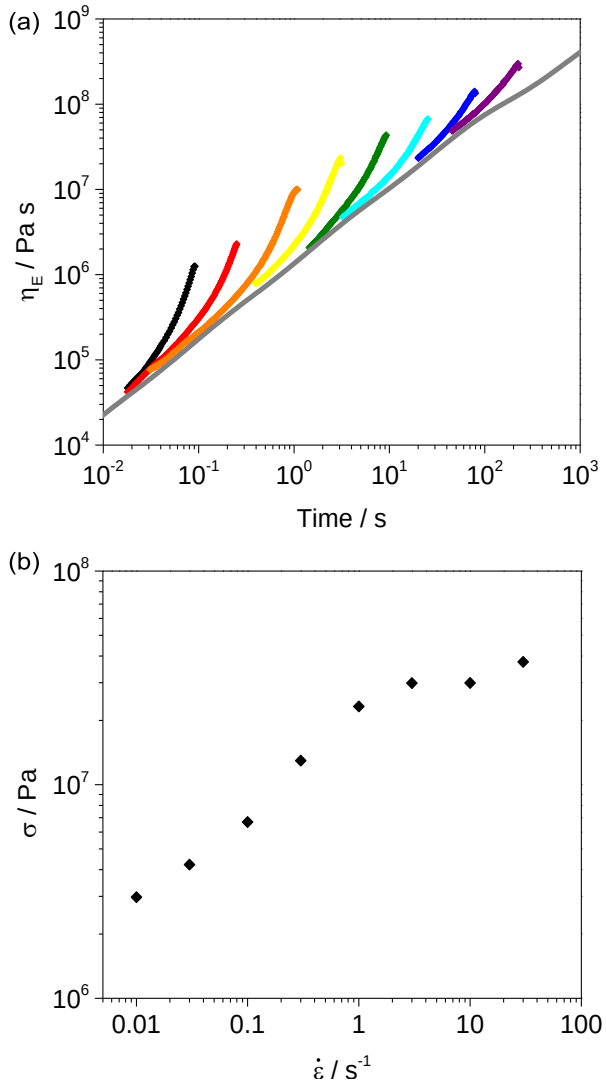

Fig. 5 (a) Extensional viscosity of UPy1, at 25 °C, at strain rates of: 30 (♦), 10 (♦), 3 (♦), 1 (♦), 0.3 (♦), 0.1 (♦), 0.03(♦) and 0.01 (♦) s^{-1}. Linear prediction of viscosity (♦). (b) Maximum extensional stress of UPy1 before sample fracture.

When $W_i \geq 1$, strain hardening occurs. If we model the supramolecular structure of UPy1 as an effective 'linear' polymer we can predict a rate at which we might expect strain hardening under extension to be observed. Using equation 3 for τ_R, it can be calculated that strain hardening would be expected for a 'linear' polymer at extension rates of 2.3 s^{-1} and above at 25 °C. Fig. 5(a) shows the extensional behaviour of UPy1 at rates from 0.01 to 30 s^{-1}. The extensional viscosity of UPy1 initially closely matches that of the prediction given by fitting Maxwell modes to the linear viscoelastic spectrum. However, at all extension rates studied the extensional viscosity then rises above this prediction, showing that the material strain-hardens under extension. Given the expectation that strain-hardening would be observed at extension rates ≥ 2.3 s^{-1} for a linear polymer, the strain hardening observed at lower extension rates shows that it is insufficient to account for this strain hardening behaviour by modelling UPy1 as a linearly assemled polymer. Strain hardening has also been observed in other self-associating polymer systems.[51,52]

In Fig. 5(b) the peak stress in UPy1 before sample fracture is plotted as a function of the extension rate. It can be seen that the stress at break increases as a function of extension rate, up until $\dot{\varepsilon} = 3$ s^{-1}, where the stress plateaus to a value of ~4×10^7 Pa. Interestingly, this coincides closely with the predicted rate at which we expect linear chain stretch to be observed, resulting in strain hardening from the linear chains. The plateau in stress above this rate suggests that the pair-pair assembly of UPy groups is being pulled apart at this stress, resulting in a brittle fracture of the sample. Similar observations were made in the work of Shabbir et al.,[53] studying brittle fracture in associative ionomers. In contrast to our work however, strain hardening was not observed in this regime. The differences in behaviour to our system seem to be a result of the different network structure and the nature of the strain hardening – where the telechelic ionomer chains bridge between clusters of counter ions. In our system the polymer assembles into much longer chains via the UPy groups. At strain rates ≤ 1 s^{-1}, where strain hardening was not expected through linear chain stretch, the stress at break is lower, but increases as a function of the strain rate. This suggests a different source for the fracturing of the polymer, such as defects brought about by thermal density fluctuations.[53] We also anticipate a further assembly of UPy groups, in addition to the linear pair-pair association, accounting for the strain hardening at these lower rates. Appel et al.[2] have shown that UPy groups are capable of further assembly, where an additional stacking interaction is seen between the cytosine alkene proton and a neighbouring dimer's pyrimidinone carbonyl group. This interaction would lead to a branched structure in the polymer chain and could explain the strain hardening behaviour at rates of 1 s^{-1} and less. Goldansaz et al.[52] have also proposed further clustering of supramolecular functional groups, beyond dimerization. This is driven by large polarity differences between the polymer chain and the functional groups, leading to a reduction in surface tension. Such weaker interactions, in comparison to the four hydrogen bonding association of pair-pair UPy assembly, explain the lower extensional stress at break if the linear polymer chain stretch had not been activated at these slower rates, while branched structures do strain harden. Because the UPy groups in our materials are connected to a bulky polymer chain, having a radius of gyration, R_g, that is far larger than the the UPy group these associations would be limited by chain stretching. This entropic penalty is rarely offset by the enthalpic gain from end-group association.[9] The stacked UPy aggregates reported for smaller functional molecules support the idea that some association to form branch points is likely but we note that large (e.g. >2 Upy dimers) aggregates are not required to contribute to strain hardening.

To determine whether or not our materials are capable of further stacking, small angle X-ray scattering measurements were undertaken at a synchrotron radiation source. The brilliance of the beam enables great sensitivity to structure within the sample, even though the scattering contrast between the UPy groups and the rest of the polymer chain is

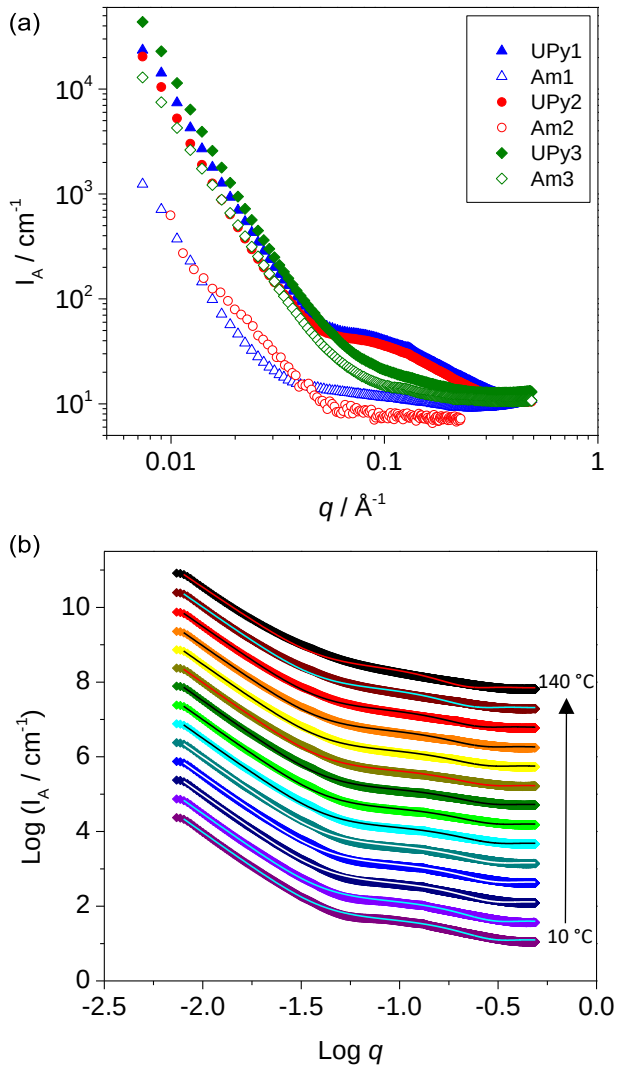

Fig. 6 Small angle X-ray scattering of UPy1, 2 and 3, and Am1, 2 and 3: (a) Scattering intensity as a function of the scattering vector, q ; (b) Fits (lines) of UPy1 at 10-140 °C using combined sphere power law model. Data staggered for clarity.

low. Fig. 6(a) shows the scattering intensity of the polymers as a function of the scattering vector, q. At low q values in the region of q < 0.04 Å^{-1}, a sharp increase in the scattering is observed for all polymer samples. The scattering can be fitted with a power law dependence of $\sim q^{-3.4--3.9}$, indicating scattering from a surface fractal with self-similar roughness. Such scattering is unexpected from these materials, and is present in both the UPy functionalised polymers and their non-functionalised counterparts. This suggests therefore that the scattering is not caused by the presence of the UPy groups. It is likely the result of polydisperse air bubbles / voids trapped within the sample, creating electron density contrast with the polymer environment.[29] At higher q values the scattering from these bubbles is greatly reduced, allowing other scattering objects to be observed. For UPy1 and UPy2 a clear shoulder to the scattering is apparent. Given the low concentration of UPy groups within the polymer melt, relative to the polymer chain length, this scattering is likely to be caused by the contrast of the UPy groups relative to the polymer chain. Am1, Am2 and Am3, which do not possess the UPy groups, show no such scattering in this region. UPy3 also has the UPy groups, but at a lower concentration than UPy1 and UPy2. No such shoulder is observed in the scattering of UPy3. It has been shown that UPy1, 2 and 3 all assemble via their UPy groups, as demonstrated by the change in rheology of these polymers (Fig. 4). Therefore, it would be expected that if the shoulder in the scattering pattern observed for UPy1 and 2 were caused by a pair-pair assembly of the UPy groups the shoulder would also be present in UPy3, albeit at a lower intensity caused by the lower concentration of UPy groups in this polymer. Therefore the shoulder present in the scattering of UPy1 and UPy2 must be from a secondary assembly of the UPy groups in the polymer, driven by the higher concentration compared to that of UPy3. The shoulder can be fitted with a sphere model, and so the scattering curves were fitted using a combined sphere power law model across the q range studied, where the scattering intensity, I, is given by:

$$I(q) = \frac{s_1}{V}\left[\frac{3V(\Delta\rho)(\sin(qr) - qr\cos(qr))}{(qr)^3}\right]^2 + s_2(q)^{-n} \quad \text{+bkg} \quad (6)$$

where s_1 and s_2 are scaling factors, V is the volume of the scattering UPy spheres, r is the radius of the scattering UPy spheres, $\Delta\rho$ is the difference in the scattering length density of the UPy groups and the PBd chains, n is the power law exponent, and bkg is the background scattering. For UPy1 and UPy2, sphere radii of 12.8 and 13.5 Å were found respectively. To test whether dissociation of the UPy groups is observed at temperatures in the region of 80-100 °C, the scattering was also measured as a function of temperature, Fig. 6(b). The sphere power law fits for UPy1 across the full temperature range are also shown. The data has been staggered for clarity,

Table 3 Fitting parameters for UPy1 and UPy2 as a function of temperature

	UPy1			UPy2		
T / °C	r / Å	s_1	n	r / Å	s_1	n
10	12.9	44.6	3.7	13.3	36.9	3.9
20	12.8	42.9	3.7	13.5	36.8	3.9
30	12.7	41.7	3.7	13.7	36.8	3.9
40	12.6	41.2	3.7	-	-	-
50	12.6	39.8	3.7	14.5	35.8	3.9
60	12.6	38.3	3.7	14.9	34.5	3.9
70	12.7	36.7	3.7	14.5	35.8	3.9
80	12.9	35.9	3.7	15.9	32.3	3.8
90	13.3	34.1	3.7	16.3	31.6	3.8
100	13.6	34.2	3.7	16.7	29.8	3.7
110	14.3	33.3	3.7	17.0	27.4	3.8
120	15.0	33.5	3.7	17.3	25.9	3.8
130	15.9	33.7	3.7	17.6	24.0	3.7
140	17.1	33.8	3.6	17.0	27.4	3.8

but clearly shows that the intensity of the shoulder observed for UPy1 reduces as the temperature is increased. The scale factor for the sphere also reduces with temperature. In addition, the radius of the sphere is seen to increase from 12.9 to 17.1 Å between 10 and 140 °C respectively. These results indicate that the concentration of the scattering objects is reducing, and that clusters of the UPy groups are breaking apart at the higher temperatures. Similar observations can be made for UPy2, as shown in Table 3.

The SAXS results show that while the NH_2 functional polymers do not form clusters, those with the UPy groups are capable of assembling into clusters through further association beyond that of pair-pair (at high enough concentrations). This could therefore lead to branch points in the architecture of the polymer, which give a characteristic strain hardening signal under extension, as has been observed for our materials.

3.1 Constitutive Modelling

Using constitutive models of polymer melts to characterise the extensional rheology, we show that strain-hardening exists in a broader regime than would be expected for linear polymers, i.e. strain-hardening occurs at lower strain-rates than would be expected for linear chains. Furthermore, by characterising the materials with models that reflect the microstructure of the material we also elicit information on this underlying topology. This modelling could then be used in combination with CFD to explore the material response in complex geometries such as those found in industrial processing. To model the rheology of these systems we use the concept of tube dynamics[54] for entangled polymers. Here any given polymer chain is confined to a tube of topological constraints made from the entanglement interactions with the surrounding chains. A polymer will relax from its tube via curvilinear diffusion along the contour of the tube in a process known as reptation. Much work on the dynamics of associative polymer systems has focused on the concepts developed in the works of Stadler, Leibler, Rubinstein and colleagues[7,8,13,55] of sticky reptation and sticky Rouse dynamics. The dynamics of the chain are modified by the associating groups which can break and reform. While sticky Rouse models are used for unentangled systems, sticky reptation is used for entangled polymers, where the polymer chain must reptate along its confining tube of entanglements. Indeed, further various works[56–59] have looked at modelling the rheology of various supramolecular polymer systems using microscale arguments for their derivation. Recently van Ruymbeke et al. have developed their time-marching algorithm model for the prediction of linear viscoelasticity[60] to supramolecular chains with sticky groups[40,61–63] and found good agreement with the linear viscoelastic features of a range of self-associating polymer architectures. Less frequently investigated is non-linear extensional rheology. Another recent paper[11] looked at extensional rheology of a UPy system finding the Upper Convected Maxwell model fits the measurements well. This system consisted of unentangled chains, whereas for the work presented here we use models derived from entanglement physics.

Given that UPy1 is capable of assembling into small clusters, as shown in the SAXS data of Fig. 6, it is likely that our system contains a mixture of both linearly associated and branched chains. Such a mixture has also been proposed in other self-associating polymer systems.[46] Therefore we have developed a model for UPy1's strain hardening behaviour under extension, to characterise such a mixture. To model our telechelic system, consisting of a polydisperse mixture of chain lengths and including branched architectures we use a combination of two constitutive models based on tube theory: (i) the Pom-pom model to capture the rheology of branching in the system and (ii) the Rolie-Poly model to capture the rheology of linearly entangled polymer chains. The two models are summarised below. We can apply the model to the non-linear extensional rheology of UPy1 and use this to characterise the architecture of the assembled structures.

The Pom-pom model[64–66] considers an ideal branched molecule consisting of a backbone connected with an equal number of q arms at each end (branch point). The model considers two fundamental timescales, namely a backbone stretch relaxation time and a backbone reptation time. Relaxation of the entangled arms is considered fast relative to the stretch and reptation time and is treated as background solvent. The stress tensor for the Pom-pom model is given as,

$$\boldsymbol{\sigma} = 3G\lambda^2\mathbf{S}$$

where **S** is the orientation tensor, λ is the backbone stretch (the length of the backbone normalised by its equilibrium value) and G is the modulus. The orientation tensor is calculated from an auxiliary tensor **A**,

$$\mathbf{S} = \frac{\mathbf{A}}{tr(\mathbf{A})},$$

where **A** is given by the Upper Convected Maxwell model with reptation time τ_b,

$$\frac{\partial \mathbf{A}}{\partial t} = \mathbf{K}.\mathbf{A} + \mathbf{A}.\mathbf{K}^T - \frac{1}{\tau_b}(\mathbf{A} - \mathbf{I}).$$

The backbone stretch evolves as,

$$\frac{\partial \lambda}{\partial t} = \lambda \mathbf{K}:\mathbf{S} - \frac{1}{\tau_S}(\lambda - 1)e^{\nu^*(\lambda-1)}, \qquad \text{for } \lambda \leq q,$$

where τ_s is the stretch relaxation time and ν^* is the strength of branch-point withdrawal and is given by $\nu^* = 2/(q-1)$. The backbone stretch is entropically limited by the amount of tension each arm can maintain before the branch-point is drawn inside the backbone tube and therefore the stretch is limited to $\lambda \leq q$.

The Rouse Linearly Entangled Polymer (Rolie-Poly) model[67,68] considers the dynamics of entangled linear chains. The model is a coarse-grained approximation of the GLaMM[67] model that considers the relaxation processes of convective constraint release, contour length fluctuations and reptation. The dynamic equation for the Rolie-Poly extra stress is given by,

$$\frac{\partial \boldsymbol{\sigma}}{\partial t} = \mathbf{K}.\boldsymbol{\sigma} + \boldsymbol{\sigma}.\mathbf{K}^T - \frac{1}{\tau_d}(\boldsymbol{\sigma} - \mathbf{I}) - \frac{2}{\tau_S}\left(1 - \sqrt{\frac{3}{T}}\right)\left[\boldsymbol{\sigma} + \beta\left(\frac{T}{3}\right)^{\delta}(\boldsymbol{\sigma} - \mathbf{I})\right],$$

where τ_d is the reptation time, τ_s is the chain retraction time, β and δ are parameters describing the convective constrain release (CCR) rate and T is the trace of the stress.

In the limit of relatively fast τ_s the model reduces to the *non-stretching* limit[68] given by,

$$\frac{\partial \boldsymbol{\sigma}}{\partial t} = \mathbf{K}.\boldsymbol{\sigma} + \boldsymbol{\sigma}.\mathbf{K}^T - \frac{1}{\tau_d}(\boldsymbol{\sigma} - \mathbf{I}) - \frac{2}{3}\mathbf{K}:\boldsymbol{\sigma}[\boldsymbol{\sigma} + \beta(\boldsymbol{\sigma} - \mathbf{I})].$$

3.2 Multimode Modelling

To capture both the transient and steady state rheological response of a material, multimode modelling is needed.[69–71] It has been shown the multimode modelling is needed to model monodisperse materials [e.g.[72]] and polydisperse materials [e.g.[70,73,74]].

The stress is modelled as a sum of modes,

$$\sigma = \sum_{i=1}^{N} G_i \sigma_i$$

where each mode has a modulus and reptation time (G_i, τ_{di}) and non-linear parameters, τ_s and q (Pom-pom).

To fit the rheology of the telechelic system we use a combination of the Pom-pom and Rolie-Poly models to capture the presence of both entangled and linear chains (fitting was performed using RepTate software[36]). The modulus and reptation time were initially fitted to the linear rheology shown in Fig. 5 (a), where the fastest mode was set to the reptation time of one sub chain and the longer relaxation times were distributed evenly on a logarithmic scale. The non-linear parameters were fitted to extensional rheology; the slowest two modes are attributed to branched molecules and fitted

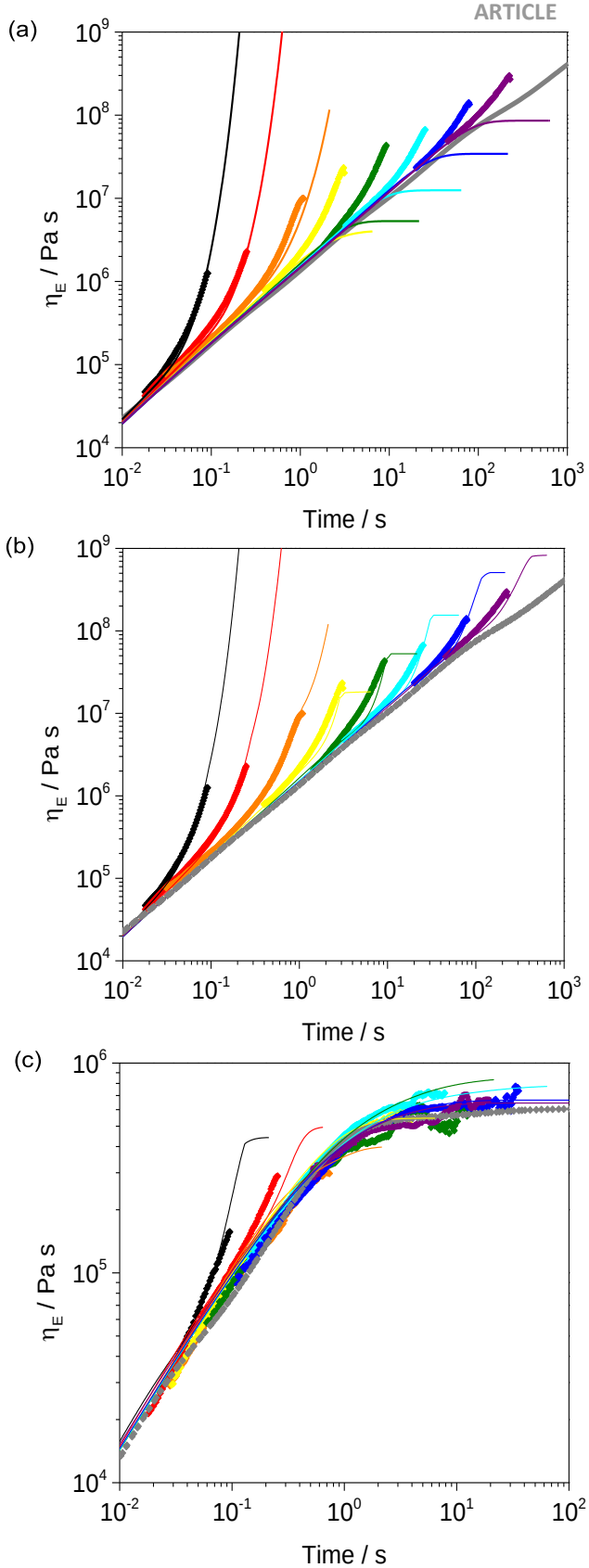

Fig. 7 Extensional viscosity of UPy1 at 25 °C ((a) and (b)) and 80 °C (c), and multi-mode modelling, at strain rates of: 30 (♦), 10 (♦), 3 (♦), 1 (♦), 0.3 (♦), 0.1 (♦), 0.03(♦) and 0.01 (♦) s^{-1}. Symbols show experimental data, lines the fits. Linear prediction of viscosity (♦). (a) The model was initially fitted using stretch Rolie-Polie modes around the relaxation times measured from linear oscillatory rheology; (b) Following the initial fit Pom-pom modes were activated for the slowest modes, allowing us to model the strain hardening behaviour across all extension rates; (c) The extensional viscosity of UPy1 was also measured at 80 °C. The model fits at 25 °C in (b) were then shifted using the TTS parameters to 80°C in (c).

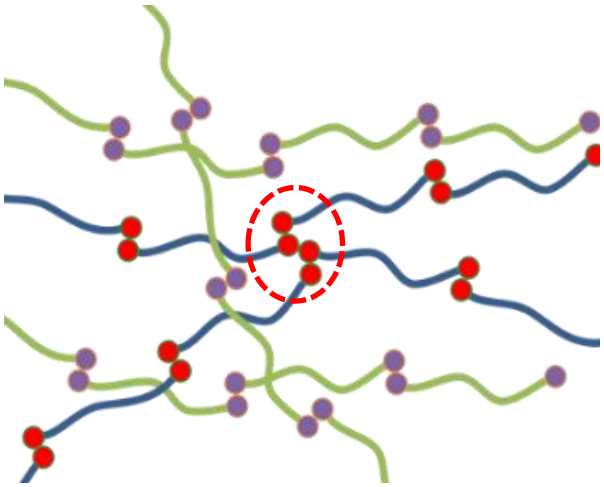

Fig. 8 Schematic of UPy assembled PBd. Green and purple chains show linearly assembled chains, blue and red shows a branched assembly of UPy groups (highlighted by circle).

using the Pom-pom model, the next three modes, fitted with the stretch Rolie-Poly model, were attributed to linear molecules of sufficient length to be stretched by the faster strain-rates, and the faster modes were assumed to orientate only and were fitted using the non-stretch Rolie-Poly model (see supporting information). The contribution of each mode towards the total complex viscosity at some given timescale and the viscosity averaged relaxation time were considered.[75] The viscosity averaged relaxation time indicates a more "real world" relaxation time that allows for the fact that some of the larger molecular weight species take longer than τ_d to relax. At 25 °C this time is 3440 s, which is longer than τ_d at 1450 s. The viscosity weighting of the branched modes was also considered. The two modes associated with branching contribute around 50% towards the LVE at long times, with the other 50% associated with linear Rolie-Poly modes. Although the inference of the precise number of branch-points is not possible at this level of analysis, the modelling does suggest that large hierarchical structures are present, which is expected for this class of material.

Fig. 7 (a) and (b) show a comparison of the multimode viscosity predictions and the experimental measurements, at 25 °C. In Fig. 7 (a) only the Rolie-Poly modes were activated, and it can be seen that these describe the strain hardening behaviour of UPy1 reasonably well at extension rates of 30, 10 and 3 s^{-1}. The initial upturn of the extensional viscosity is slightly below that of the experimental data, however. Below these rates the Rolie-Poly prediction is strain softening, where the stretch times of the polymer are too fast to lead to strain hardening. This also matches our prediction that the linearly assembled polymer chains would strain harden at rates above ≥ 2.3 s^{-1} but not below. To describe the strain hardening behaviour at these slower rates therefore it is necessary to activate Pom-pom modes as the slowest three modes as described above. By activating these modes we are now able to get good fits for all extension rates studied, as shown in Fig. 7(b). In Fig. 7 (c) the extensional data of UPy1 at 80 °C is shown. At extension rates of 30 and 10 s^{-1} the extensional viscosity of UPy1 rises above that of the linear viscoelastic prediction, showing strain hardening even at this raised temperature. At extension rates below this however the measured extensional viscosity closely matches that of the linear viscoelastic prediction, with no strain hardening. The extensional viscosity of the polymer plateaus as the time scale of the experiment goes beyond that of its reptation time. The multi-mode modelling of the extensional data at 25 °C has been shifted using the TTS parameters of the polymer to 80 °C and is also shown in Fig. 7 (c). A good agreement with the experimental data is observed and shows that at 80 °C there remain branched clusters of UPy groups that lead to strain hardening of UPy1. As a further observation we note that since our Pom-pom model fits the data over a range of strain-rates then the branch-points that exist must be stable over these timescales. We note that it is possible for individual branch-points to break and re-associate, but if there are sufficiently many of them then on average the material will behave as if it is branched, which the experimental data confirms is the case.

Using this method we have been able to successfully describe the rheological behaviour of the UPy functionalised PBd as a mixture of both linearly associated and branched assemblies, which result in a huge extension to the terminal relaxation time of the polymer, an increase in the plateau modulus of the polymer, and extensional strain hardening. Fig. 8 displays a schematic of the self-assembled polymer structures formed by the UPy functionalised PBds.

Conclusions

Polybutadienes telechelically functionalised with the multiple-hydrogen bonding UPy group were studied to determine the effect of functionalisation on the viscoelastic properties of the polymers. The terminal relaxation time of the functionalised polymers was extended by several orders of magnitude, driven by the assembly of the UPy groups. The temperature at which the terminal relaxation cross-over was observed at a frequency of 1 Hz was found to be between 80-100 °C for the three UPy functionalised polymers, regardless of molecular weight and chain microstructure, and was linked to dissociation of the UPy groups. The non-linear behaviour of UPy1 was investigated under extension and was found to strain harden across the extension rate range studied of 0.01 – 30 s^{-1}. We found strain hardening would be expected at rates ≥ 2.3 s^{-1} through chain stretch for a linearly assembled polymer but not below. Therefore, we anticipated the assembly of a secondary structure by the UPy groups. SAXS confirmed the presence of small clusters of ~2.5 nm in diameter for UPy1 and UPy2, but not UPy3. This was attributed to the lower concentration of UPy groups in UPy3, because of the longer polymer chain length. Because of this clustering we developed a constitutive model combining the Pom-Pom and Rolie-Poly models to fit the non-linear extensional rheology of UPy1. We were able to use this model to characterise the system as a mixture of linear chains assembled by pair-pair UPy hydrogen bonding, and branched

chains resulting from the formation of UPy clusters. The average cluster lifetime must be > 100 s, given the strain hardening at rates of 0.01 s^{-1}.

Conflicts of interest

There are no conflicts to declare.

Acknowledgements

We thank Michelin Research, Clermont-Ferrand for supporting this work. We thank Diamond Light Source for access to beamline I22 (SM8440) that contributed to the results presented here. This work benefited from the use of the SasView application, originally developed under NSF award DMR-0520547.

Notes and references

1 L. Yang, X. Tan, Z. Wang and X. Zhang, *Chem. Rev.*, 2015, **115**, 7196–7239.
2 W. P. J. Appel, G. Portale, E. Wisse, P. Y. W. Dankers and E. W. Meijer, *Macromolecules*, 2011, **44**, 6776–6784.
3 H. Kautz, D. J. M. van Beek, R. P. Sijbesma and E. W. Meijer, *Macromolecules*, 2006, **39**, 4265–4267.
4 K. Yamauchi, J. R. Lizotte, D. M. Hercules, M. J. Vergne and T. E. Long, *J. Am. Chem. Soc.*, 2002, **124**, 8599–8604.
5 M. Müller, U. Seidel and R. Stadler, *Polymer (Guildf).*, 1995, **36**, 3143–3150.
6 F. J. Stadler, W. Pyckhout-Hintzen, J.-M. Schumers, C.-A. Fustin, J.-F. Gohy and C. Bailly, *Macromolecules*, 2009, **42**, 6181–6192.
7 R. Stadler, *Prog. Colloid Polym. Sci.*, 1987, **75**, 140–145.
8 L. Leibler, M. Rubinstein and R. H. Colby, *Macromolecules*, 1991, **24**, 4701–4707.
9 F. Ishiwari, G. Okabe, H. Ogiwara, T. Kajitani, M. Tokita, M. Takata and T. Fukushima, *J. Am. Chem. Soc.*, 2018, **140**, 13497–13502.
10 A. Jangizehi, S. R. Ghaffarian, W. Schmolke and S. Seiffert, *Macromolecules*, 2018, **51**, 2859–2871.
11 G. Cui, V. A. H. Boudara, Q. Huang, G. P. Baeza, A. J. Wilson, O. Hassager, D. J. Read and J. Mattsson, *J. Rheol. (N. Y. N. Y).*, 2018, **62**, 1155–1174.
12 E. Van Ruymbeke, *J. Rheol. (N. Y. N. Y).*, 2017, **61**, 1099–1102.
13 M. Rubinstein and A. N. Semenov, *Macromolecules*, 2001, **34**, 1058–1068.
14 N. E. Botterhuis, D. J. M. van Beek, G. M. L. van Gemert, A. W. Bosman and R. P. Sijbesma, *J. Polym. Sci. Part A Polym. Chem.*, 2008, **46**, 3877–3885.
15 J. Cortese, C. Soulié-Ziakovic, M. Cloitre, S. Tencé-Girault and L. Leibler, *J. Am. Chem. Soc.*, 2011, **133**, 19672–5.
16 M. Dionisio, L. Ricci, G. Pecchini, D. Masseroni, G. Ruggeri, L. Cristofolini, E. Rampazzo and E. Dalcanale, *Macromolecules*, 2014, **47**, 632–638.
17 Y. Yang and M. W. Urban, *Chem. Soc. Rev.*, 2013, **42**, 7446–7467.
18 P. Cordier, F. Tournilhac, C. Soulié-Ziakovic and L. Leibler, *Nature*, 2008, **451**, 977–80.
19 L. R. Hart, J. L. Harries, B. W. Greenland, H. M. Colquhoun and W. Hayes, *Polym. Chem.*, 2013, **4**, 4860–4870.
20 K. Yamauchi, J. R. Lizotte and T. E. Long, *Macromolecules*, 2003, **36**, 1083–1088.
21 A. W. Bosman, R. P. Sijbesma and E. W. Meijer, *Mater. Today*, 2004, **7**, 34–39.
22 C. Heinzmann, C. Weder and L. M. de Espinosa, *Chem. Soc. Rev.*, 2016, **45**, 342–358.
23 Y. Zhang, C. A. Anderson and S. C. Zimmerman, *Org. Lett.*, 2013, **15**, 3506–9.
24 C. A. Anderson, A. R. Jones, E. M. Briggs, E. J. Novitsky, D. W. Kuykendall, N. R. Sottos and S. C. Zimmerman, *J. Am. Chem. Soc.*, 2013, **135**, 7288–95.
25 L. Zhang, N. R. Brostowitz, K. A. Cavicchi and R. A. Weiss, *Macromol. React. Eng.*, 2014, **8**, 81–99.
26 F. J. Stadler, T. Still, G. Fytas and C. Bailly, *Macromolecules*, 2010, **43**, 7771–7778.
27 J. Cortese, C. Soulié-Ziakovic, S. Tencé-Girault and L. Leibler, *J. Am. Chem. Soc.*, 2012, **134**, 3671–3674.
28 F. Herbst, K. Schröter, I. Gunkel, S. Gröger, T. Thurn-Albrecht, J. Balbach and W. H. Binder, *Macromolecules*, 2010, **43**, 10006–10016.
29 M. Krutyeva, A. R. Brás, W. Antonius, C. H. Hövelmann, A. S. Poulos, J. Allgaier, A. Radulescu, P. Lindner, W. Pyckhout-Hintzen, A. Wischnewski and D. Richter, *Macromolecules*, 2015, **48**, 8933–8946.
30 C. L. Lewis, K. Stewart and M. Anthamatten, *Macromolecules*, 2014, **47**, 729–740.
31 R. P. Sijbesma, F. H. Beijer, L. Brunsveld, B. J. B. Folmer, J. H. K. K. Hirschberg, R. F. M. Lange, J. K. L. Lowe and E. W. Meijer, *Science (80-.).*, 1997, **278**, 1601–1604.
32 S. H. M. Söntjens, R. P. Sijbesma, M. H. P. van Genderen and E. W. Meijer, *J. Am. Chem. Soc.*, 2000, **122**, 7487–7493.
33 A. Louhichi, A. R. Jacob, L. Bouteiller and D. Vlassopoulos, *J. Rheol. (N. Y. N. Y).*, 2017, **61**, 1173–1182.
34 P. J. Woodward, D. H. Merino, B. W. Greenland, I. W. Hamley, Z. Light, A. T. Slark and W. Hayes, *Macromolecules*, 2010, **43**, 2512–2517.
35 http://www.sasview.org.
36 J. Ramirez, V. A. H. Boudara and D. J. Read, Rheology of Entangled Polymers: Toolbox for the Analysis of Theory and Experiments, https://reptate.readthedocs.io/index.html.
37 M. L. Williams, R. F. Landel and J. D. Ferry, *J. Am. Chem. Soc.*, 1955, **77**, 3701–3707.
38 M. Müller, A. Dardin, U. Seidel, V. Balsamo, B. Iván, H. W. Spiess and R. Stadler, *Macromolecules*, 1996, **29**, 2577–2583.
39 A. E. Likhtman and T. C. B. McLeish, *Macromolecules*, 2002, **35**, 6332–6343.
40 E. Van Ruymbeke, D. Vlassopoulos, M. Mierzwa, T. Pakula, D. Charalabidis, M. Pitsikalis and N. Hadjichristidis, *Macromolecules*, 2010, **43**, 4401–4411.
41 B. J. Gold, C. H. Hövelmann, N. Lühmann, W. Pyckhout-

Hintzen, A. Wischnewski and D. Richter, *J. Rheol. (N. Y. N. Y).*, 2017, **61**, 1211–1226.
42 Z. Zhang, C. Huang, R. A. Weiss and Q. Chen, *J. Rheol. (N. Y. N. Y).*, 2017, **61**, 1199–1207.
43 A. Shabbir, I. Javakhishvili, S. Cerveny, S. Hvilsted, A. L. Skov, O. Hassager and N. J. Alvarez, *Macromolecules*, 2016, **49**, 3899–3910.
44 S. Seiffert, *Macromol. Rapid Commun.*, 2016, **37**, 257–264.
45 J. L. Viovy, M. Rubinstein and R. H. Colby, *Macromolecules*, 1991, **24**, 3587–3596.
46 W. H. Tuminello, *Polym. Eng. Sci.*, 1986, **26**, 1339–1347.
47 C. Tsenoglou, *Macromolecules*, 1991, **24**, 1762–1767.
48 J. Des Cloizeaux, *Macromolecules*, 1990, **23**, 3992–4006.
49 L. J. Fetters, D. J. Lohse and R. H. Colby, in *Physical Properties of Polymers Handbook*, ed. J. E. Mark, AIP Press, New York, 1996, pp. 335–340.
50 F. T. Trouton, *Proc. R. Soc. London. Ser. A, Contain. Pap. a Math. Phys. Character*, 1906, **77**, 426–440.
51 A. Shabbir, H. Goldansaz, O. Hassager, E. van Ruymbeke and N. J. Alvarez, *Macromolecules*, 2015, **48**, 5988–5996.
52 H. Goldansaz, C.-A. Fustin, M. Wübbenhorst and E. van Ruymbeke, *Macromolecules*, 2016, **49**, 1890–1902.
53 A. Shabbir, Q. Huang, Q. Chen, R. H. Colby, N. J. Alvarez and O. Hassager, *Soft Matter*, 2016, **12**, 7606–7612.
54 M. Doi and S. F. Edwards, *The Theory of Polymer Dynamics*, Clarendon Press, Oxford, 1986.
55 R. Stadler and L. de Lucca Freitas, *Macromolecules*, 1989, **22**, 714–719.
56 S. Wang and R. G. Larson, *J. Rheol. (N. Y. N. Y).*, 2018, **62**, 477–490.
57 T. Furuya and T. Koga, *J. Polym. Sci. Part B Polym. Phys.*, 2018, **56**, 1251–1264.
58 S. Lalitha Sridhar and F. Vernerey, *Polymers (Basel).*, 2018, **10**, 848.
59 L. Martinetti, O. Carey-De La Torre, K. S. Schweizer and R. H. Ewoldt, *Macromolecules*, 2018, **51**, 8772–8789.
60 E. Van Ruymbeke, R. Keunings and C. Bailly, *J. Nonnewton. Fluid Mech.*, 2005, **128**, 7–22.
61 E. van Ruymbeke, K. Orfanou, M. Kapinstos, H. Iatrou, M. Pitsikalis, N. Hadjichristidis, D. J. Lohse and D. Vlassopoulos, *Macromolecules*, 2007, **40**, 5941–5952.
62 M. Ahmadi, L. G. D. Hawke, H. Goldansaz and E. Van Ruymbeke, *Macromolecules*, 2015, **48**, 7300–7310.
63 F. Zhuge, L. G. D. Hawke, C.-A. Fustin, J.-F. Gohy and E. van Ruymbeke, *J. Rheol. (N. Y. N. Y).*, 2017, **61**, 1245–1262.
64 T. C. B. McLeish and R. G. Larson, *J. Rheol. (N. Y. N. Y).*, 1998, **42**, 81.
65 R. J. Blackwell, T. C. B. McLeish and O. G. Harlen, *J. Rheol. (N. Y. N. Y).*, 2000, **44**, 121–136.
66 T. C. B. McLeish, *Adv. Phys.*, 2002, 51, 1379–1527.
67 R. S. Graham, A. E. Likhtman, T. C. B. McLeish and S. T. Milner, *J. Rheol. (N. Y. N. Y).*, 2003, **47**, 1171.
68 A. E. Likhtman and R. S. Graham, *J. Nonnewton. Fluid Mech.*, 2003, **114**, 1–12.
69 N. J. Inkson, T. C. B. McLeish, O. G. Harlen and D. J. Groves, *J. Rheol. (N. Y. N. Y).*, 1999, 43, 873.
70 T. D. Lord, L. Scelsi, D. G. Hassell, M. R. Mackley, J. Embery, D. Auhl, O. G. Harlen, R. Tenchev, P. K. Jimack and M. A. Walkley, *J. Rheol. (N. Y. N. Y).*, 2010, **54**, 355.
71 D. W. Auhl, D. M. Hoyle, D. G. Hassell, T. D. Lord, M. R. Mackley, O. G. Harlen and T. C. B. McLeish, *J. Rheol. (N. Y. N. Y).*, 2011, **55**, 875.
72 M. W. Collis, A. K. Lele, M. R. Mackley, R. S. Graham, D. J. Groves, A. E. Likhtman, T. M. Nicholson, O. G. Harlen, T. C. B. McLeish, L. R. Hutchings, C. M. Fernyhough and R. N. Young, *J. Rheol. (N. Y. N. Y).*, 2005, **49**, 501.
73 D. G. Hassell, T. D. Lord, L. Scelsi, D. H. Klein, D. Auhl, O. G. Harlen, T. C. B. McLeish and M. R. Mackley, *Rheol. Acta*, 2011, **50**, 675–689.
74 D. M. Hoyle, D. Auhl, O. G. Harlen, V. C. Barroso, M. Wilhelm and T. C. B. McLeish, *J. Rheol. (N. Y. N. Y).*, 2014, **58**, 969–997.
75 D. M. Hoyle, University of Leeds, 2010.

